Brazilian Journal of Geophysics, **41** (2023), 1, 61–74
Brazilian Geophysical Society
ISSN 2764-8044
DOI 10.22564/brjg.v41i1.2296

NUMERICAL SIMULATION OF 2D SEISMIC WAVE PROPAGATION IN ISOTROPIC AND ANISOTROPIC MEDIA APPLIED TO A ZERO-OFFSET VSP OF THE ISLEÑO FIELD, EASTERN VENEZUELA BASIN

Richard Perez-Roa [1,2*], Mario Caicedo [3], and Ginette Lagrave [4]

[1]Yachay Tech University, School of Earth Sciences, Energy and Environment, Hacienda San José, Urcuquí, Ecuador
[2]Universidad Central de Venezuela, Graduate Program in Physics, Science Faculty, Caracas, Venezuela
[3]Universidad Simón Bolívar, Department of Physics, Caracas, Venezuela
[4]PDVSA Petrodelta, Superintendence of Integrated Reservoir Studies, Maturin, Venezuela

*Corresponding author: rperez@yachaytech.edu.ec

ABSTRACT. For a full wave inversion, it plays an important role to know the medium (isotropic, anisotropic, poroelastic etc.) that best fits the observed data. Therefore, the goal of this work, which is part of a larger FWI project, is to study which direct problem allows us to better describe the set of observed data available to us. To this end, 2D numerical simulations of seismic wave propagation were carried out using a staggered grid finite difference approach to simulate the acquisition of a zero-offset VSP. The synthetic data (d) were compared with the data (dobs) of a zero-offset VSP acquired in the Isleño field, Greater Temblador Area in the Monagas State, Venezuela. The physical models studied were wave propagation in isotropic and VTI anisotropic media. The results of the study show three aspects to stake. First, the signal decay for the vertical component of both the real and simulated data is similar. Second, when comparing the vertical component of the real and synthetic data, it is observed that, for a signal recorded at 996 m, the correlation was 0.75 for the isotropic medium and 0.81 for the VTI anisotropic medium for direct waves. Finally, the third, the comparison for the horizontal component recorded at the same depth shows a correlation of 0.40 for the isotropic medium model and 0.34 for the VTI anisotropic medium for direct waves. The results obtained allow us to deduce that in the case of performing a full wave inversion in the land seismic data acquired in the Isleño field, it is recommended that it be of the anisotropic full wave inversion type to obtain better results.

Keywords: numerical simulation, seismic wave propagation, isotropy, VTI anisotropy.

INTRODUCTION

The numerical simulation of seismic data and its comparison with real ones has been carried out at different scales, starting at small scales, as for example Bretaudeau et al. (2011); Pageot et al. (2017); Solymosi et al. (2018). There are also examples of the application of synthetic modeling of acoustical propagation applied to seismic oceanography experiments (Kormann et al., 2010) for the quantification of site effects (Chávez-García et al., 2000), as well as for the quality control of high-resolution reflection seismic methods as non-destructive tool for engineering tasks (Burschil et al., 2015). However, no examples of the use of numerical simulation of seismic data and its comparison with real data at a zero-offset Vertical Seismic Profile (VSP) have been found in the scientific literature to investigate which type of medium (isotropic or anisotropic) best fits actual seismic data.

A geophysical inversion process seeks to indirectly extract information from the medium of the observed

data, which is why it is necessary to have an equation or system of equations that best describes the relationship between the environment and the observed data. The process of mapping the parameters of a geological model to quantities in the data space is known as forward modeling, generally of the type (Tarantola, 2005):

$$d = F(m), \tag{1}$$

where **d** is the observed data and **F** is the function that relates the parameters of the medium **m** with the observed data. For the particular case of Full Waveform Inversion (FWI): it is a high-resolution seismic imaging technique that is based on the use of all the content of the seismic traces, which have little or no null processing, to extract the physical parameters of the medium sampled by the seismic waves. However, like any seismic inversion method, it needs to use a theory that satisfactorily relates the physical parameters of the medium with the observed data. For this, the objective of this work, as part of a larger FWI project, it was analyzed which theory best describes the observed seismic data. So, in this work, 2D numerical simulations of seismic wave propagation were performed using a staggered grid finite difference method for a zero-offset VSP acquisition case. The results were compared with the data from a zero-offset VSP acquired in the Isleño field, Greater Temblador Area in Monagas State, Venezuela. The theories that were analyzed were those of wave propagation in isotropic and VTI anisotropic media to determine which theory best describes the observed data, in order to, when the FWI of the land seismic data of the Isleño field is carried out, select which equations for the direct problem will give better results.

STUDY AREA

The Isleño Field is located in the Southwestern sector of the Uracoa Municipality of Monagas State and northeast of the Orinoco Oil Belt. From a geological point of view, it forms part of the southern flank of the Maturín sub-basin in the Eastern Venezuela Basin. It is located approximately 8 km south of Uracoa Field and 30 km southeast of the city of Temblador (Fig. 1) (CVET, 1970).

This zone is tectonically characterized by a passive margin with the transgressive influence of the interaction zone between the Caribbean and the South American plates. This interaction generated foreland-type depocenters and folds thrusts in the deformation front, resulting in the creation of the Barinas-Apure and the Eastern Venezuela Basins, where the study field is located. From west to east, the Oriental basin is divided into two sub-basins: the Guárico and the Maturín sub-basins, separated by the Urica and Anaco fault systems (CVET, 1970). The stratigraphy of the fields of the area is characteristic of the southern zone of the Eastern Venezuela basin and all fields in the area are very stratigraphically similar, composed by four large sedimentary units: the Mesa, Las Piedras, Freites, and Oficina Formations which unconformably cover a Cretaceous sedimentary unit, the Temblador Group (Fig. 1b). This entire sequence lies on a Precambrian igneous metamorphic basement that represents the northern edge of the Guayana shield (CVET, 1970).

ELASTIC WAVE EQUATIONS FOR ISOTROPIC AND VTI ANISOTROPIC MEDIA

Elastic waves are disturbances that propagate through a medium and are characterized by their ability to transmit energy without transporting matter. When a disturbance occurs in the medium, either through an external force or a generating source, these waves are produced (Caicedo and Mora, 2004).

In an isotropic medium, elastic waves propagate in all directions with the same velocity and amplitude. This means that the elastic properties of the medium are the same in all directions. For an elastic and isotropic medium in a 2D Cartesian system with the horizontal and positive x-axis to the right and the positive z-axis downwards, the P-SV equations of motion in the velocity-stress scheme are (Virieux, 1986):

$$\begin{aligned}
\frac{\partial v_x}{\partial t} &= \frac{1}{\rho}\left(\frac{\partial \sigma_{xx}}{\partial x} + \frac{\partial \sigma_{xz}}{\partial z}\right) \\
\frac{\partial v_z}{\partial t} &= \frac{1}{\rho}\left(\frac{\partial \sigma_{xz}}{\partial x} + \frac{\partial \sigma_{zz}}{\partial z}\right) \\
\frac{\partial \sigma_{xx}}{\partial t} &= (\lambda + 2\mu)\frac{\partial v_x}{\partial x} + \lambda\frac{\partial v_z}{\partial z} \\
\frac{\partial \sigma_{zz}}{\partial t} &= \lambda\frac{\partial v_x}{\partial x} + (\lambda + 2\mu)\frac{\partial v_z}{\partial z} \\
\frac{\partial v_x z}{\partial t} &= \mu\left(\frac{\partial v_x}{\partial z} + \frac{\partial v_z}{\partial x}\right)
\end{aligned} \tag{2}$$

Where v_x, v_z is the velocity vector; $\sigma_{xx}, \sigma_{zz}, \sigma_{xz}$ is the stress tensor; ρ is the density; and λ and μ are Lame's constants.

On the other hand, in a VTI anisotropic medium, the elastic properties of the medium vary with direction. Elastic waves propagate at different velocities and with different amplitudes depending on the direction in which they propagate. The equations of movement for a VTI anisotropic medium are given by (Etgen, 1988; Caicedo and Mora, 2004):

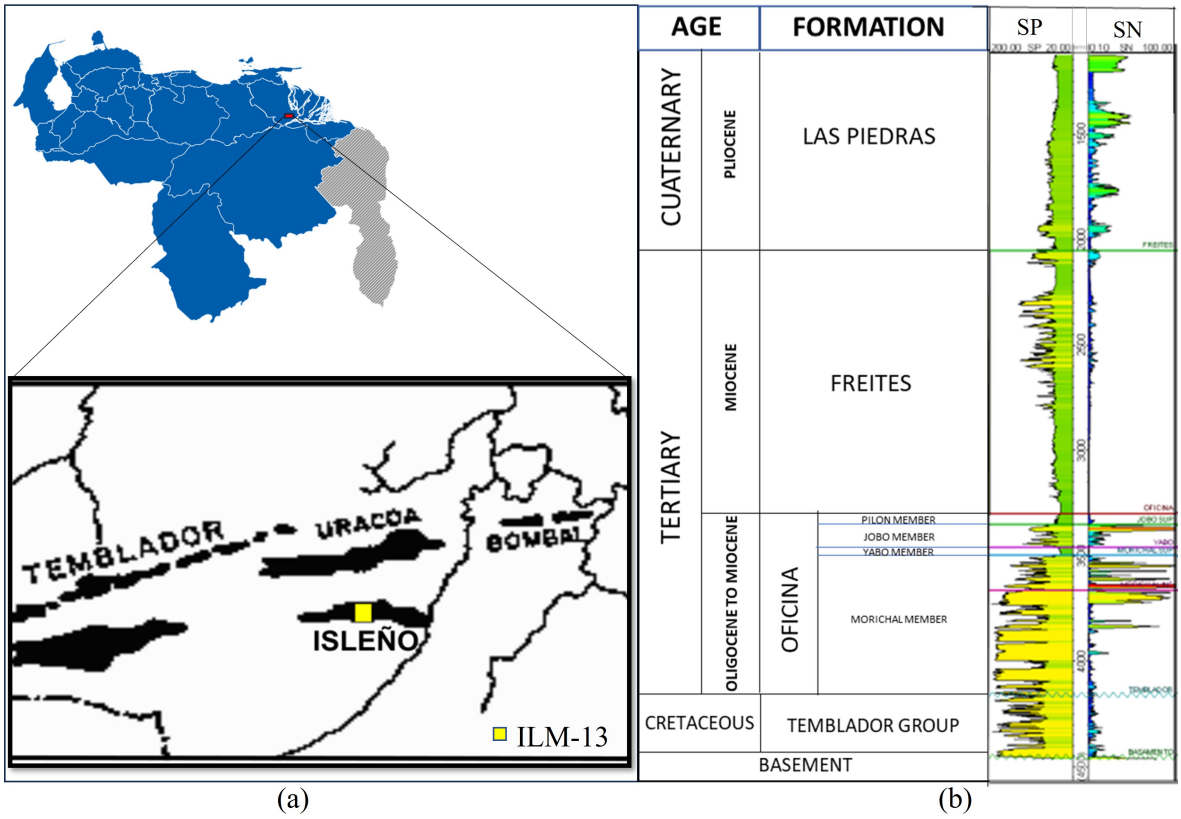

Figure 1: (a) Geographic location of the Isleño Field. The ILM-13 well where the zero-offset VSP was acquired is in the yellow box; (b) Stratigraphic Column of Isleño Field area.

$$
\begin{aligned}
\frac{\partial v_x}{\partial t} &= \frac{1}{\rho}\left(\frac{\partial \sigma_{xx}}{\partial x} + \frac{\partial \sigma_{xz}}{\partial z}\right) \\
\frac{\partial v_z}{\partial t} &= \frac{1}{\rho}\left(\frac{\partial \sigma_{xz}}{\partial x} + \frac{\partial \sigma_{zz}}{\partial z}\right) \\
\frac{\partial \sigma_{xx}}{\partial t} &= C_{11}\frac{\partial v_x}{\partial x} + C_{13}\frac{\partial v_z}{\partial z} \\
\frac{\partial \sigma_{zz}}{\partial t} &= C_{13}\frac{\partial v_x}{\partial x} + C_{33}\frac{\partial v_z}{\partial z} \\
\frac{\partial v_x z}{\partial t} &= C_{44}\left(\frac{\partial v_x}{\partial z} + \frac{\partial v_z}{\partial x}\right)
\end{aligned}
\tag{3}
$$

where C_{11}, C_{13}, C_{33} and C_{44} are the elastic coefficients for a vertical transverse isotropy (VTI) medium.

STAGGERED GRID FINITE DIFFERENCES IN THE TIME DOMAIN

The first implementations of the finite difference method in a seismological context used a conventional grid where all field variables (e.g., displacement, stress and strain) are defined at the same grid positions, as e.g. Kelly et al. (1976).

The breakthrough in finite difference modeling was the application of the staggered grid approach to discretization, where some of the wave quantities are defined on a reference grid, and the rest of the quantities are defined on a step grid, which is the offset grid midpoint of the reference grid (Fig. 2). This technique was proposed by Madariaga (1976) and was used to model an expanding circular fault.

MATHERIALS AND METHODS

Two cases were analyzed for the 2D numerical simulation of the propagation of seismic waves. The first case assumed the medium as isotropic and in the second case it was used a VTI anisotropic medium. For the numerical simulation for the isotropic medium, the records of P wave velocity (V_P), S wave velocity (V_S), density (ρ); and for the numerical simulation of the VTI anisotropic medium, in addition to the aforementioned records, it was also used the clay volume record (VCL), from the weak elastic anisotropy parameters of Thomsen, to make the calculation. Figure 3 shows a diagram of the methodology used in this work.

In the ILM-13 well, a zero-offset VSP (ZVSP) was acquired at the interval 29.87 m – 1070.20 m MD using the VSI tool. The frequency analysis shows a frequency content of 8-90 Hz and noise above 95 Hz. For the ZVSP, a Vibroseis truck was used as a source and the source was at 33.53 m and at an azimuth of 210° from the well. 66 levels were acquired between 29.87 m and 1070.18 m in measured depth (MD). Then,

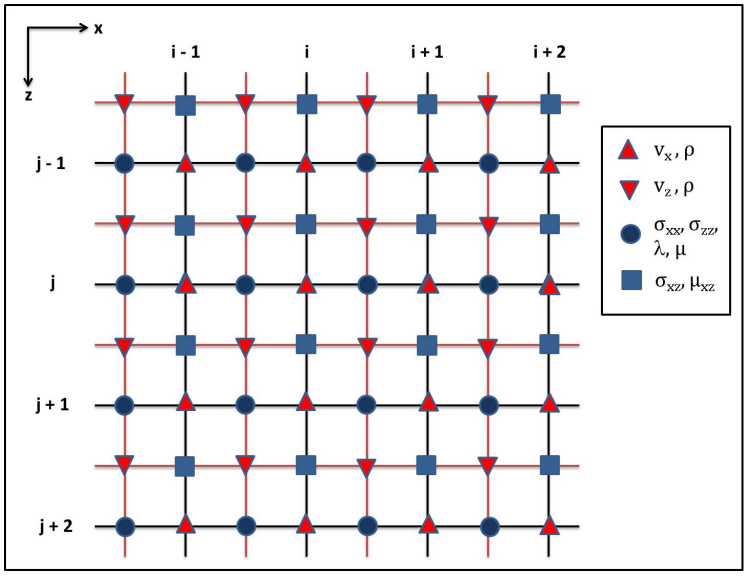

Figure 2: Spatial discretization for the 2D problem in continuous isotropic medium.

from the well logs and the acquisition configuration, grids of the input parameters necessary for the simulations with values of $\Delta x = \Delta z = 0.999744m$ were constructed as shown in Figure 4. The medium is assumed to be perfectly horizontal since the dip in the study area is approximately 4°.

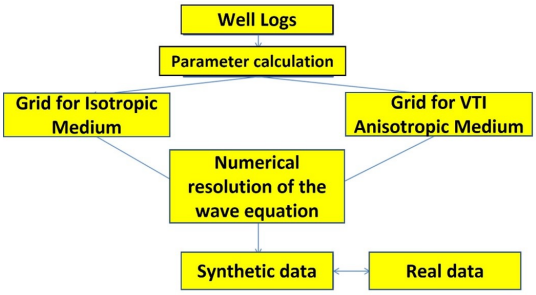

Figure 3: Methodology used in this work.

The values of λ and μ required in the numerical simulation for an isotropic medium were calculated from V_P, V_S and ρ using the following equations:

$$\begin{aligned} \lambda &= \rho(V_P^2 - 2V_S^2) \\ \mu &= \rho V_S^2 \end{aligned} \tag{4}$$

For numerical simulation in a VTI anisotropic medium, the values of the coefficients C_{11}, C_{13}, C_{33} and C_{44} are needed and are calculated from the following equations (Thomsen, 1986; Yilmaz, 2001):

$$C_{33} = \rho(V_P^2) \tag{5}$$

$$C_{44} = \rho(V_S^2) \tag{6}$$

$$C_{11} = C_{33}(2\varepsilon + 1) \tag{7}$$

$$C_{13} = \sqrt{2\delta C_{33}(C_{33} - C_{44}) + (C_{33} - C_{44})^2} - C_{44} \tag{8}$$

where ε and δ are known as Thomsen's elastic weak anisotropic parameters (Thomsen, 1986). These parameters were calculated from the VCL using the empirical equations proposed by Li (2006):

$$\varepsilon = \frac{0,60VCL(V_P - V_{Pwater})}{V_{Pquartz} - V_{Pwater} - 2,65VCL} \tag{9}$$

$$\delta = 0.32\varepsilon \tag{10}$$

where $V_{Pwater} = 1.50km/s$ and $V_{Pquartz} = 6.05km/s$. The time interval used was $\Delta t = 0.04ms$ and the total recording time was $1.75s$. The wavelet used was the one obtained from the autocorrelation of the Vibroseis sweep used as a source in the acquisition (Fig. 5).

RESULTS AND ANALYSIS

The first thing that was done was to compare the decay of the signal of the vertical component v_z of the real data with respect to those obtained for the numerical simulation in the isotropic medium and the VTI anisotropic medium, showing the results obtained in Figure 6.

As observed in the results obtained, the decay of the signal amplitude for the vertical component v_z is similar for both the real and the synthetic data obtained in the numerical simulations.

Next, Figure 7 shows the seismogram for the vertical component v_z of the real data and Figure 8 shows the seismograms of the synthetic data obtained from the numerical simulations for the isotropic and VTI anisotropic media. It can be seen that the arrival time for the first arrival is similar for the real and for the simulated data.

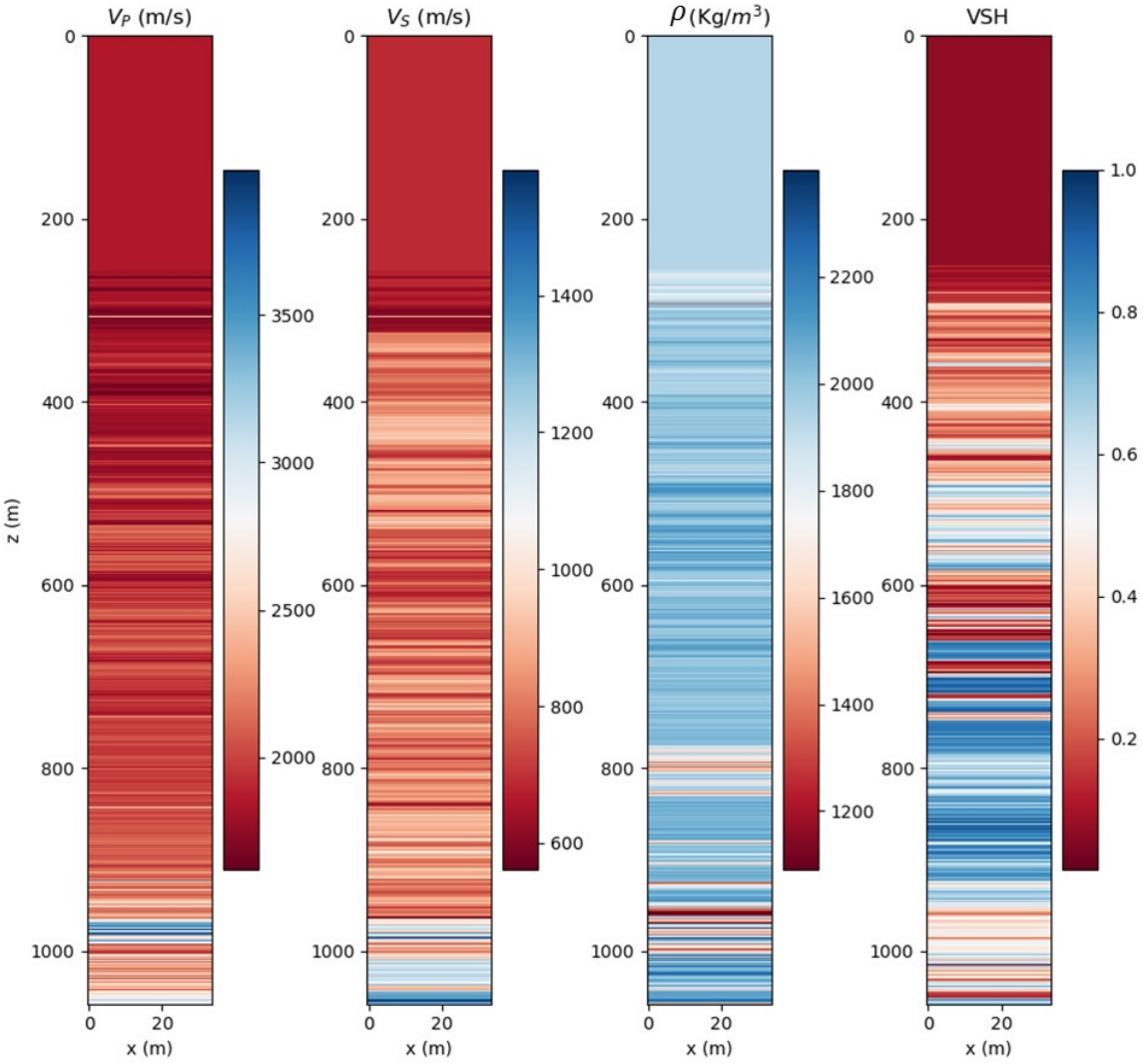

Figure 4: Grids of V_P, V_S, ρ and VCL used in the numerical simulations.

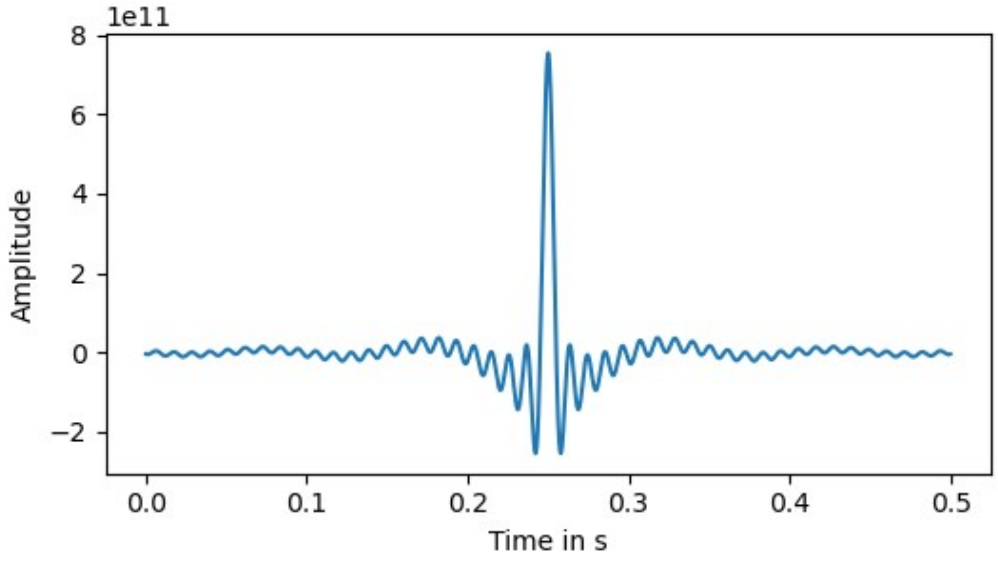

Figure 5: Source wavelet used for the numerical simulations of the ZVSP in the ILM-13 well.

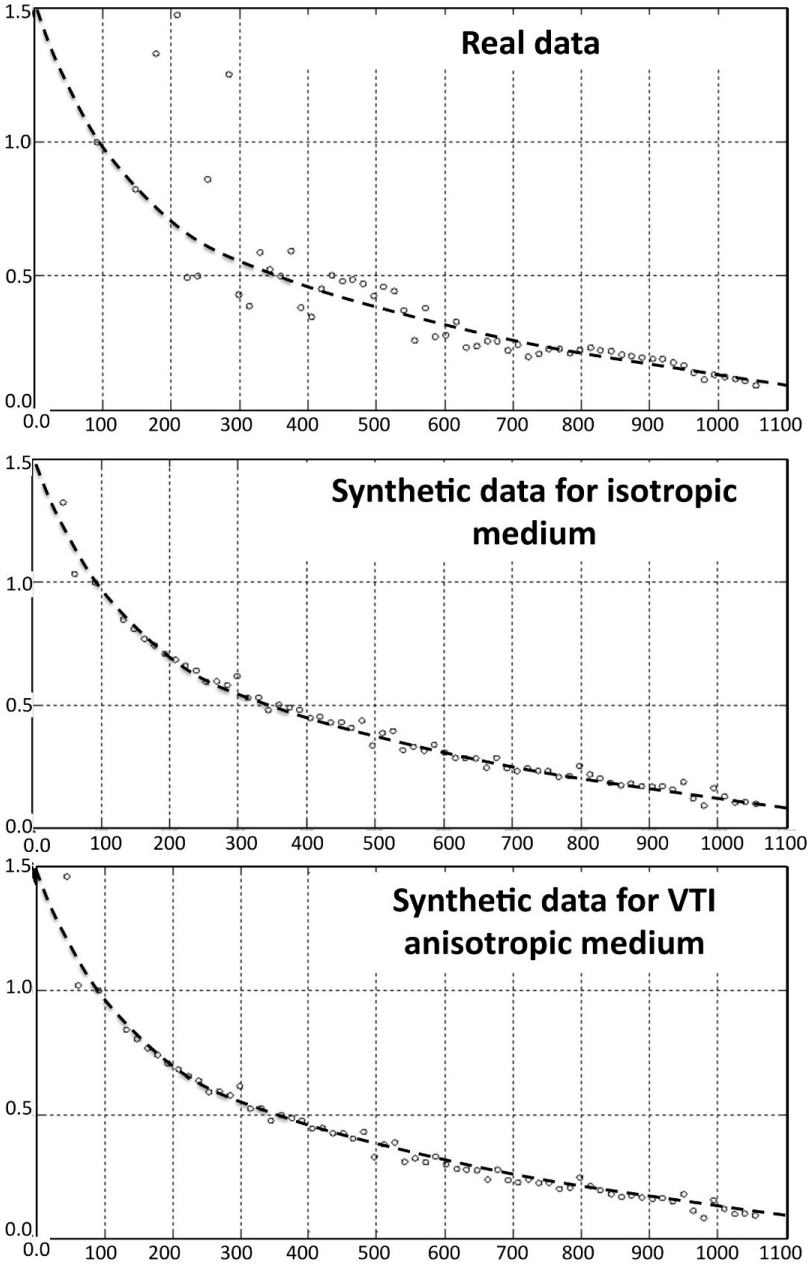

Figure 6: Decay of the v_z signal of the real and of the synthetic data for the isotropic and the VTI anisotropic media.

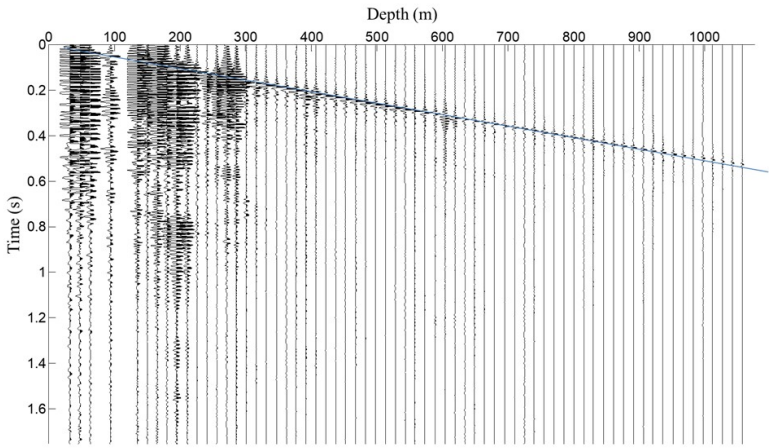

Figure 7: Seismogram for the vertical component v_z of the real data.

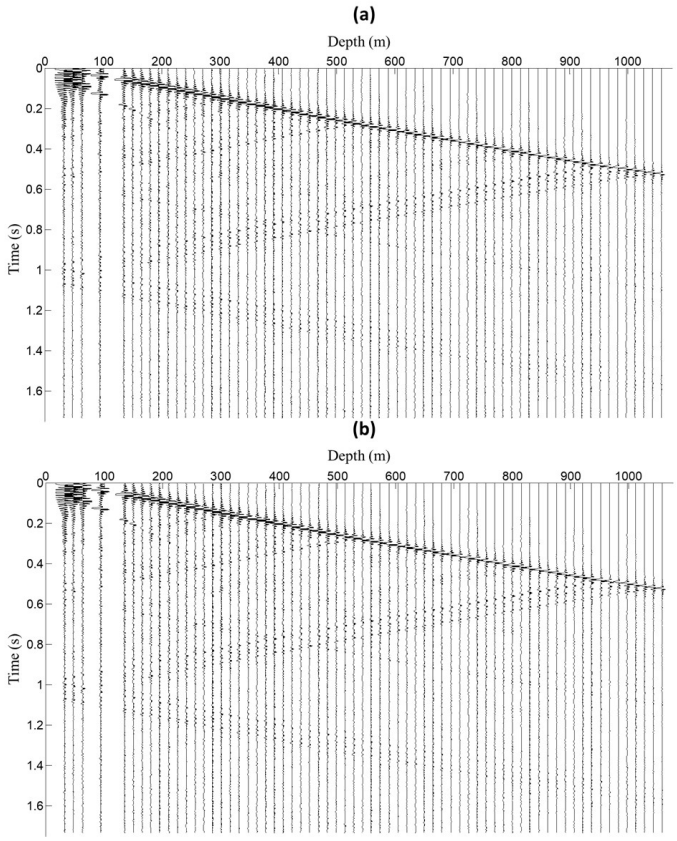

Figure 8: Seismogram for the vertical component v_z of the synthetic data resulting from the numerical simulation: (a) isotropic medium (b) VTI anisotropic medium.

Continuing, the signal that was recorded at 996 m was selected and compared with what was obtained in the numerical simulation for an isotropic medium (Fig. 9) and for a VTI anisotropic medium (Fig. 10). If we visually analyze the comparison between the real and the simulated signals of the isotropic medium, a good adjustment is observed in valleys and peaks and in the amplitude for times from $0.30s$ to $0.75s$, but after this time it is observed a considerable difference in amplitude, as the real signal decays to values close to zero, while the simulated signal remains between -0.10 and 0.10. Then the correlation between the observed and calculated seismic components for the v_z component of the isotropic medium was analyzed. A separation of direct reflection windows $(0 - 0.75s)$ and primary reflections $(0.75\breve{}1.7s)$ was made. The correlation obtained for the window of $0 - 0.75s$ was 0.75 and the resulting correlation for the window of $0.75 - 1.7s$ was 0.03, that is, it can be said that the correlation is null for this last interval. Then a correlation factor was calculated in a moving window with a width of $100ms$ as a function of the reflection time which is shown in Figure 11.

Regarding the comparison between the real data and the results obtained for the VTI anisotropic medium, if we visually analyze it, similar results are observed as those obtained for the isotropic medium, that is, a good fit in valleys and peaks and in amplitude, for times from $0.30sto0.75s$. However, after this time, a considerable difference in amplitude is observed since the real signal decays to values close to zero. In contrast, the simulated signal remains between -0.10 and 0.10. If quantitatively compared the correlation between the observed and calculated seismic components for the component of the VTI anisotropic medium, similar to the isotropic medium, the analysis shows a separation of direct reflection windows $(0 - 0.75s)$ and primary reflections $(0.75\breve{}1.7s)$. The correlation obtained for the window of $0 - 0.75s$ was 0.81 and the resulting correlation for the window of $0.75 - 1.7s$ was -0.11, which means that the correlation is null for this last interval. Then a correlation factor was calculated in a moving window with a width of $100ms$ as a function of the reflection time which is shown in Figure 12.

Now we will see and analyze the results obtained for the horizontal component v_x. Figure 13 shows the seismogram for the horizontal component v_x of the real data and Figure 14 shows the seismograms for the synthetic data obtained from the numerical simulations of the isotropic and VTI anisotropic media as well as for the vertical component. It can be observed that the arrival time for the first arrival is similar for the real and the simulated data.

Then we selected the signal that was recorded for the horizontal component v_x at 996 m in the same way that we did for the vertical component v_z and it was compared with what was obtained in the numerical simulation for an isotropic (Fig. 15) and for a VTI anisotropic medium (Fig. 16). If we visually analyze the comparison between the real and the simulated signals of the isotropic medium, it is observed that the amplitudes are similar for the times from $0.30sto0.70s$. However, a good fit between the valleys and real peaks is not observed. Moreover, the simulated ones, after $0.70s$, a considerable difference in amplitude is observed since the real signal decays to values close to zero while the simulated signal remains approximately between -0.20 and 0.20 and if they are compared quantitatively the correlation between the observed and calculated seismic components for the v_x component of the isotropic medium was analyzed, a separation of direct reflection windows $(0 - 0.75s)$ and primary reflections $(0.75\breve{}1.7s)$ was made, the correlation obtained for the window of $0 - 0.75s$ was 0.40 and for the window of $0.75 - 1.7s$ the resulting correlation was 0.19, that is, it can be said that the correlation is low for this last interval. Then a correlation factor was calculated in a moving window with a width of $100ms$ as a function of the reflection time which is shown in Figure 17.

As for the comparison between the real data and the results obtained for the VTI anisotropic medium, if we analyze it visually, similar results are observed as those obtained for the isotropic medium, that is, it is observed that the amplitudes are similar for the times of $0.40sto1.00s$ but a good fit is not observed between

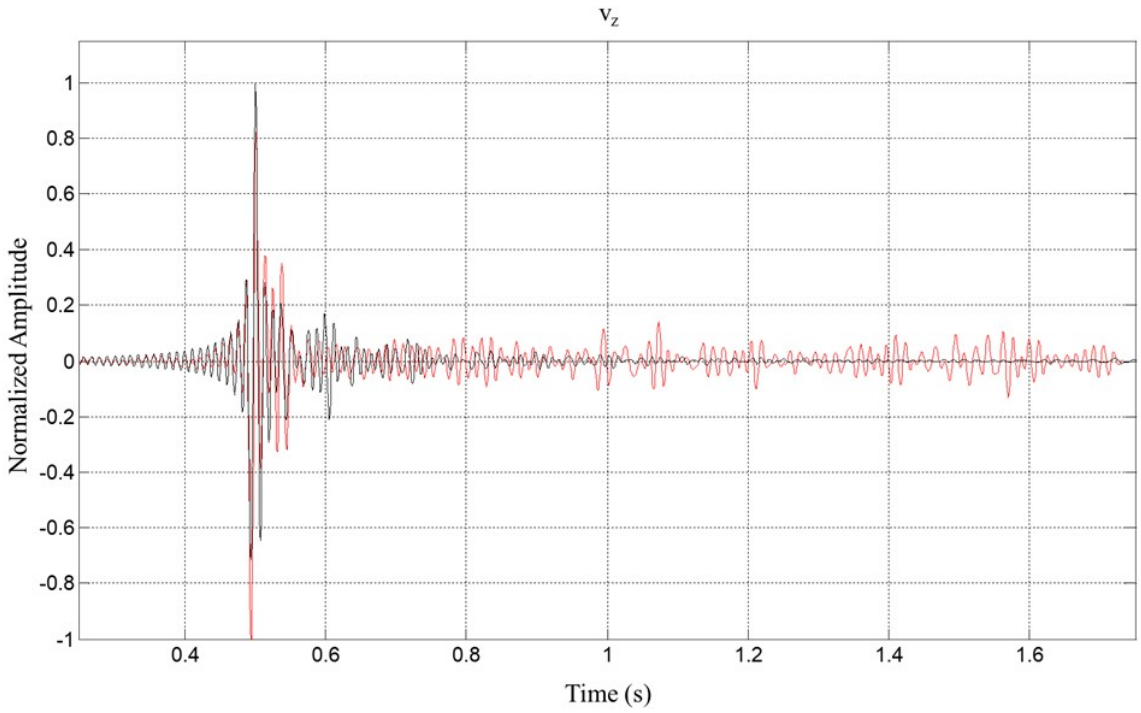

Figure 9: Comparison for the signal of the vertical component v_z of the real (black line) and the synthetic (red line) data resulting from the numerical simulation for an isotropic medium in the signal recorded at 996 m.

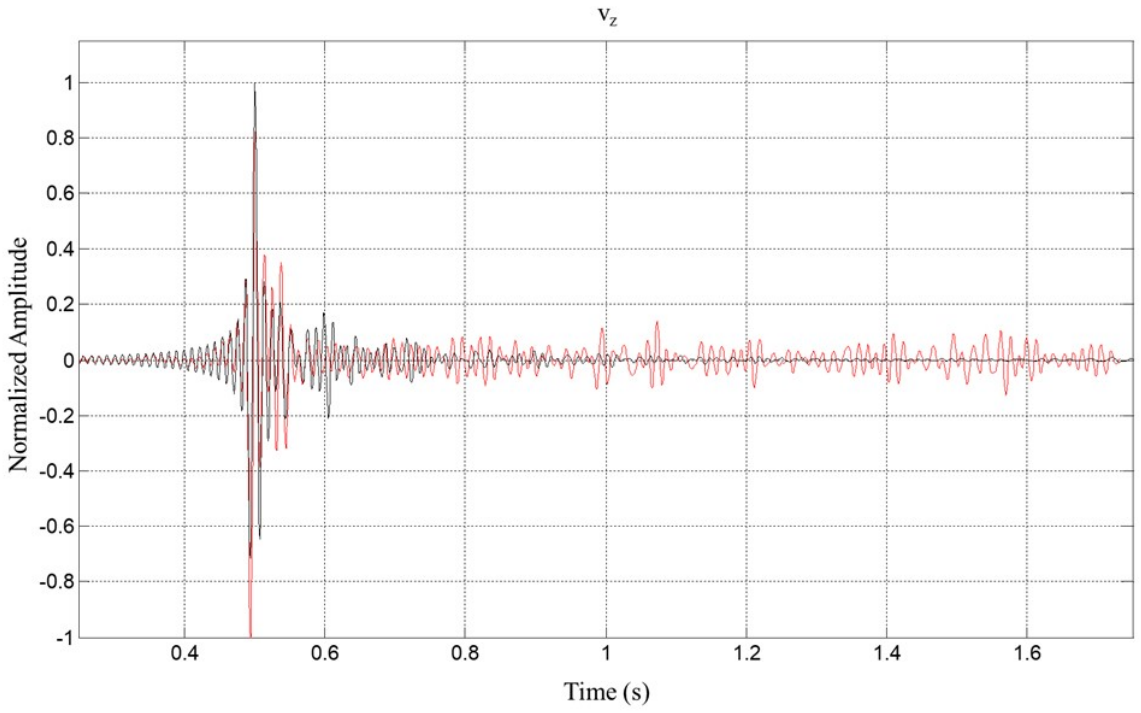

Figure 10: Comparison for the signal of the vertical component v_z of the real (black line) and the synthetic (red line) data resulting from the numerical simulation for a VTI anisotropic medium in the signal recorded at 996 m.

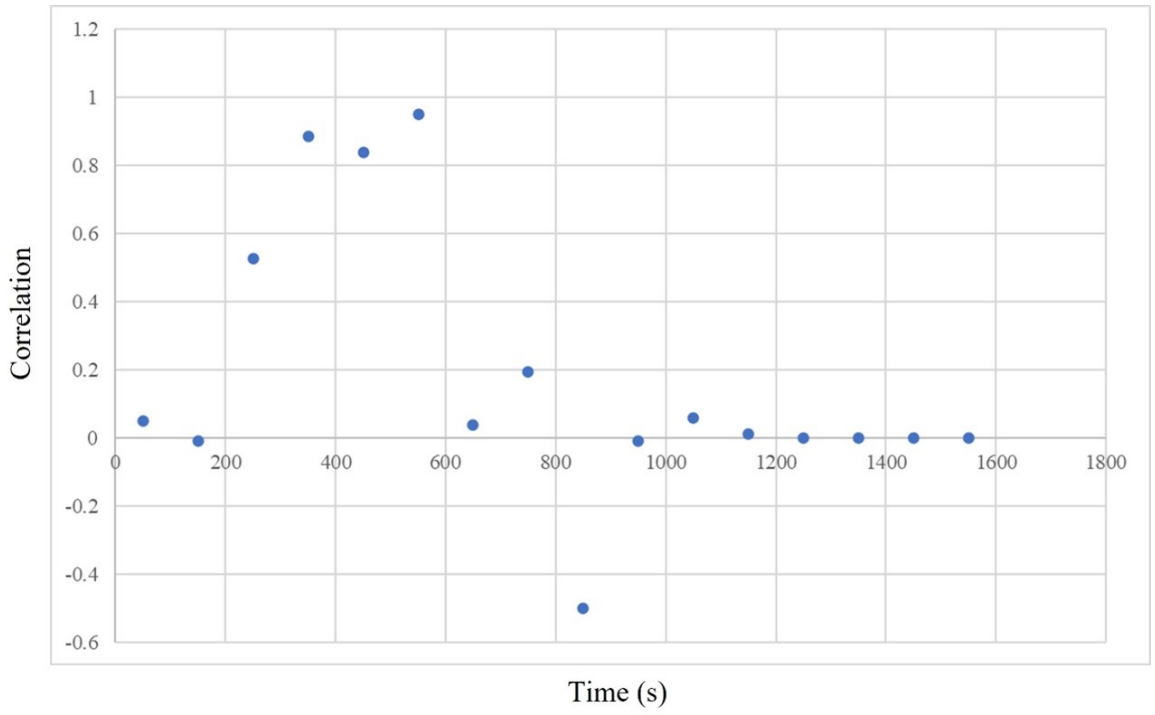

Figure 11: Correlation factor for a moving window of $100ms$ for the v_z component of an isotropic medium. Note that the highest correlation values occur in the interval $0.3 - 0.6s$.

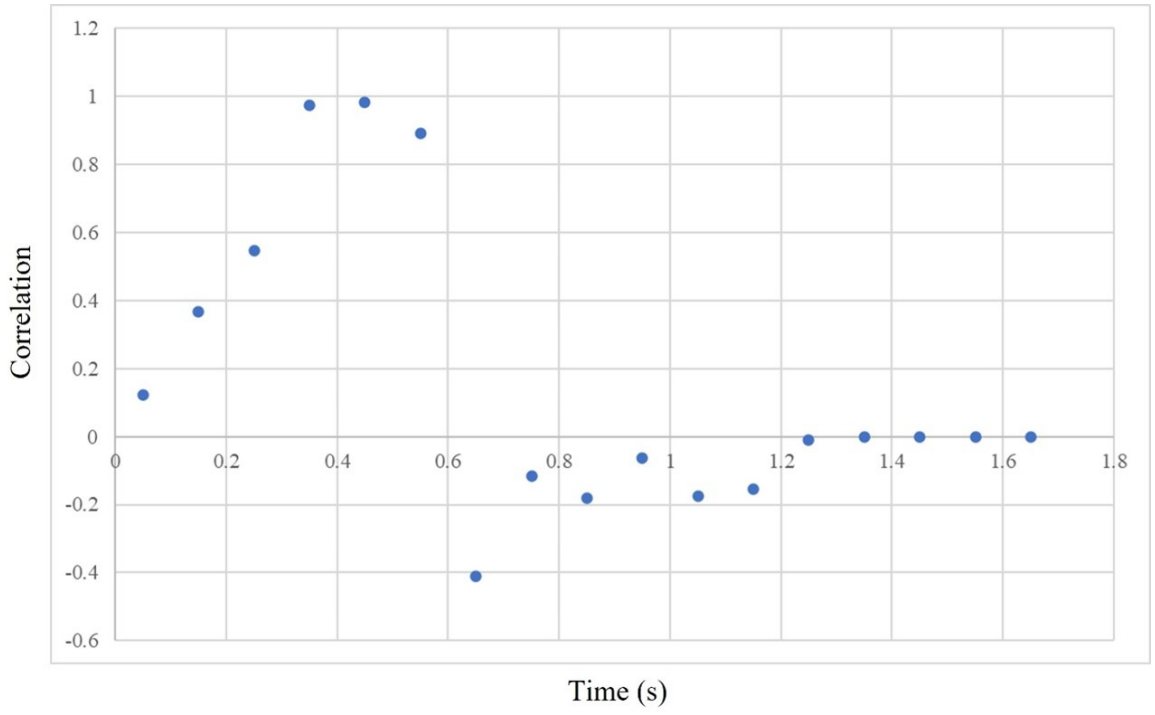

Figure 12: Correlation factor for a moving window of $100ms$ for the v_z component of a VTI anisotropic medium. Note that the highest correlation values occur in the interval $0.3 - 0.6s$.

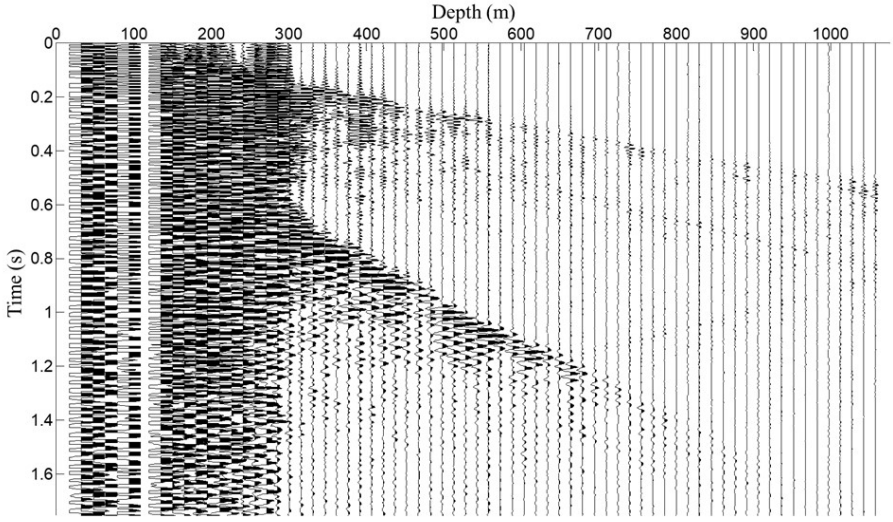

Figure 13: Seismogram for the horizontal component v_x of the real data.

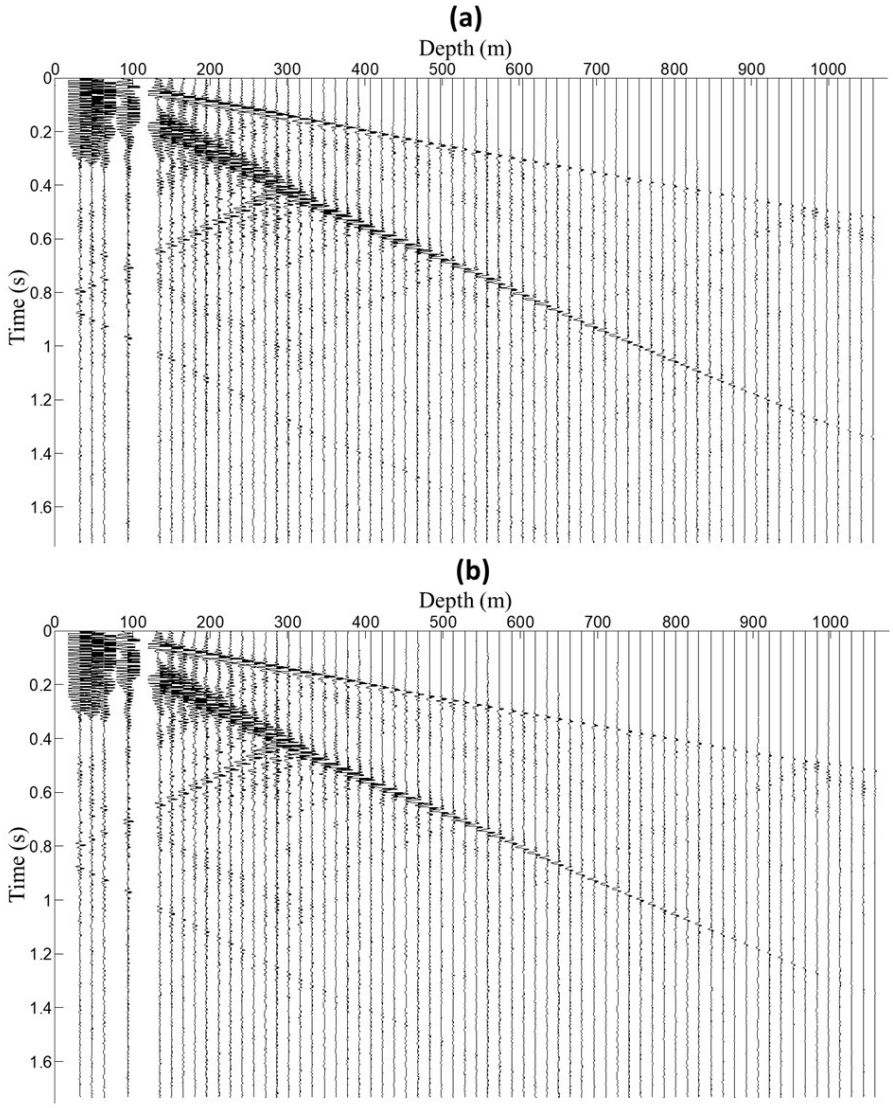

Figure 14: Seismogram for the horizontal component v_x of the synthetic data resulting from the numerical simulation: (a) isotropic medium (b) VTI anisotropic medium.

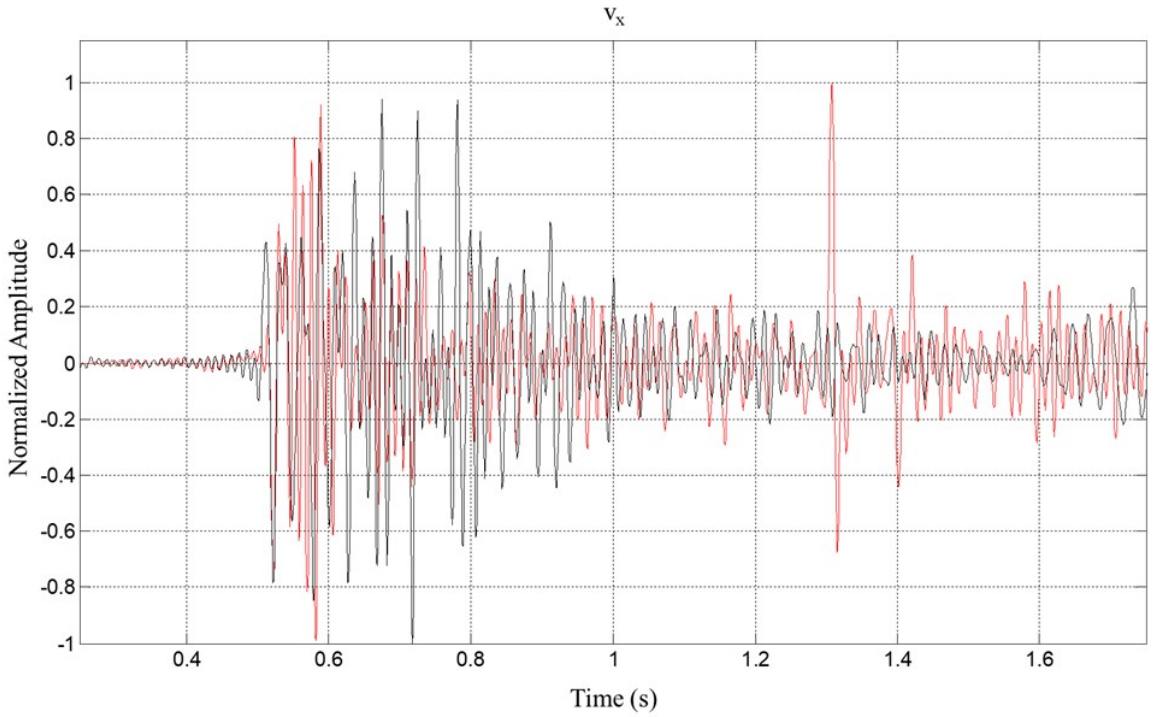

Figure 15: Comparison for the signal of the horizontal component v_x of the real (black line) and the synthetic (red line) data resulting from the numerical simulation for an isotropic medium in the signal recorded at 996 m.

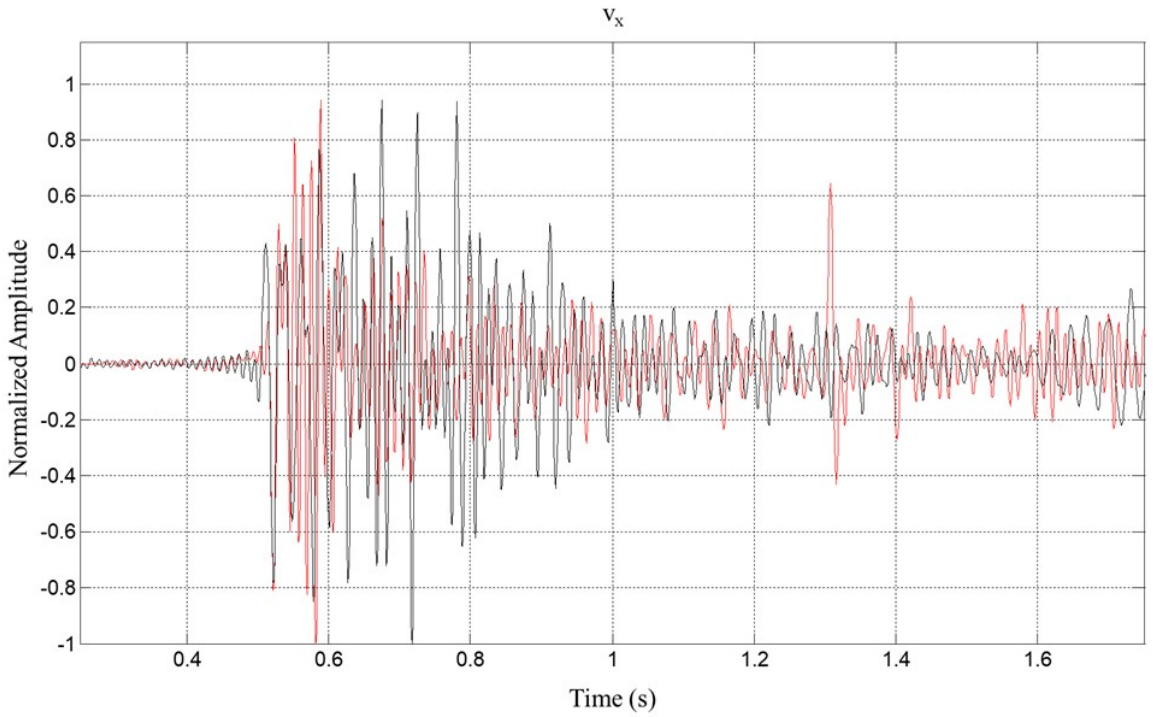

Figure 16: Comparison for the signal of the horizontal component v_x of the real (black line) and the synthetic (red line) data resulting from the numerical simulation for a VTI anisotropic medium in the signal recorded at 996 m.

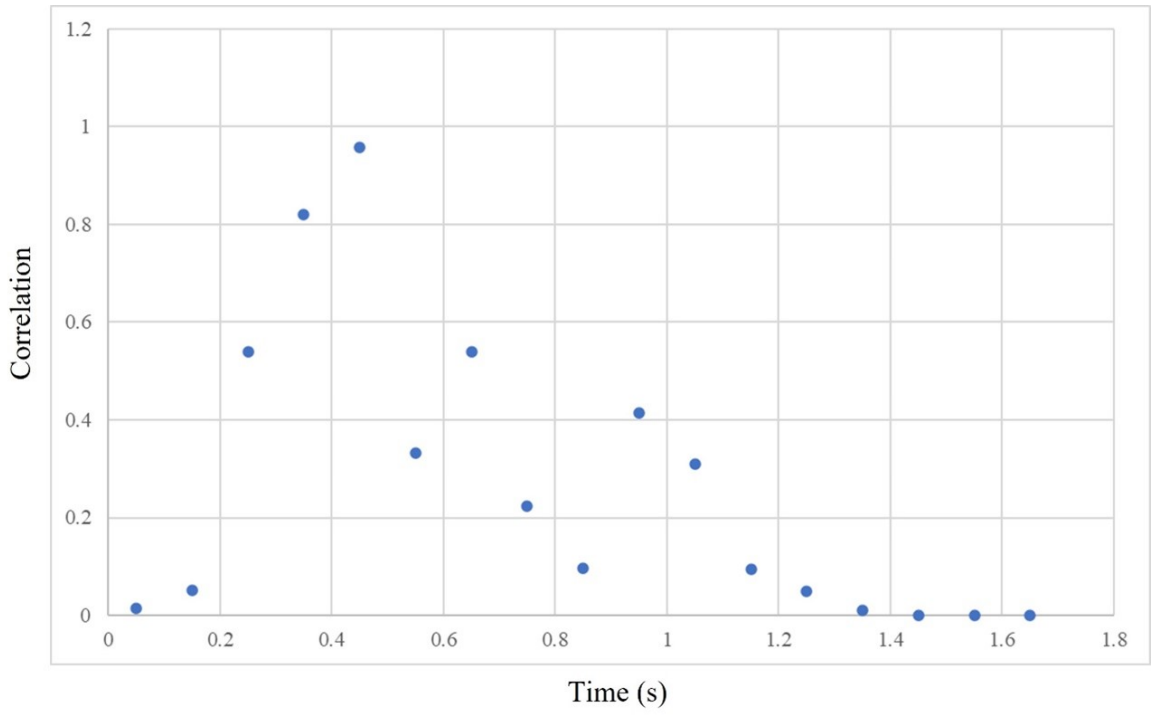

Figure 17: Correlation factor for a moving window of $100ms$ for the v_x component of an isotropic medium. Note that the highest correlation values occur in the interval $0.3 - 0.7s$.

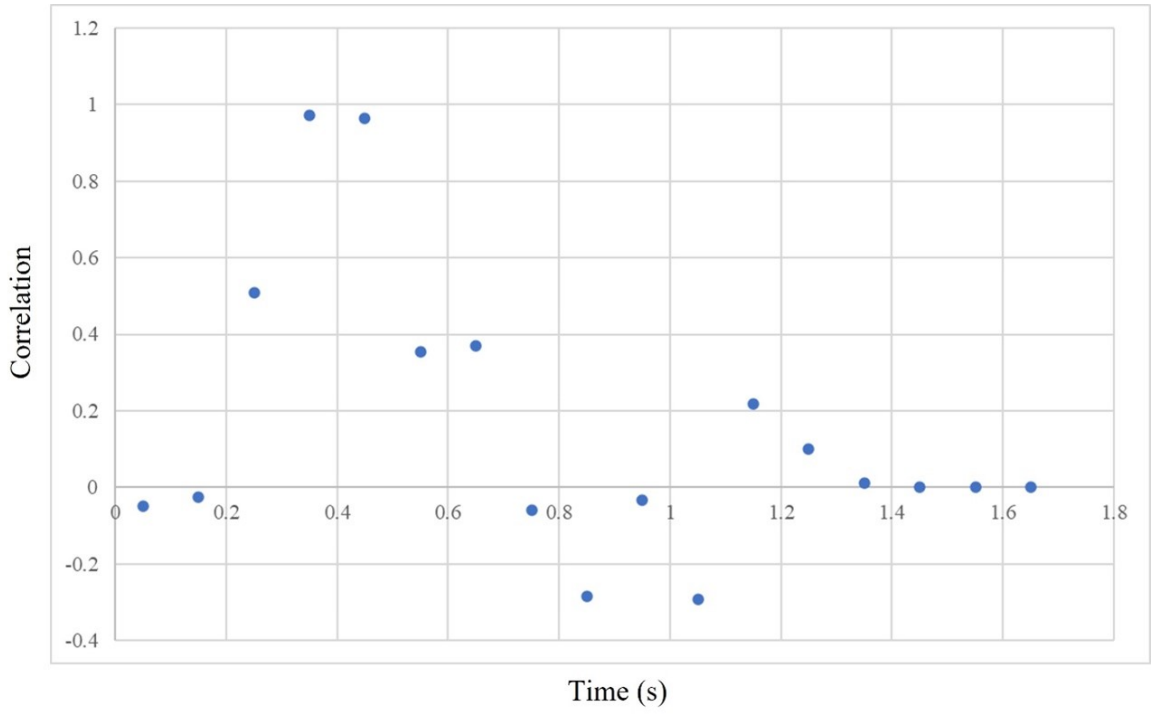

Figure 18: Correlation factor for a moving window of $100ms$ for the v_x component of a VTI anisotropic medium. Note that the highest correlation values occur in the interval $0.3 - 0.7s$.

the real and simulated valleys and peaks. After $1.00s$, a considerable difference in amplitude is observed since the real signal decays to values close to zero, while the simulated signal remains approximately between -0.20 and 0.20. If quantitatively compared the correlation between the observed and calculated seismic components for the component of the VTI anisotropic medium, similar to the isotropic medium, it is observed a separation of direct reflection windows $(0 - 0.75s)$ and primary reflections $(0.75\check{}1.7s)$. The correlation obtained for the window of $0 - 0.75s$ was 0.34 and the resulting correlation for the window of $0.75 - 1.7s$ was -0.09, which means that the correlation is null for this last interval. Then a correlation factor was calculated in a moving window with a width of $100ms$ as a function of the reflection time which is shown in Figure 18.

DISCUSSION

In isotropic media, the properties of the medium remain consistent in all directions. This implies that seismic waves propagate at the same velocity regardless of their propagation direction. Comparing the simulation results with the actual data, it is evident that the accuracy of the vertical component (v_z) is higher than that of the horizontal component (v_x).

On the other hand, in VTI anisotropic media, the properties of the medium vary with the direction of the wave propagation. This means that the velocity of the seismic wave propagation depends on the direction in which the wave travels (Thomsen, 1986). Similar to the numerical simulations conducted for the isotropic medium, the results indicate that the vertical component (v_z) performs better than the horizontal one (v_x).

If we focus solely on v_z, we observe that the similarities are more pronounced in the VTI anisotropic medium compared to the isotropic medium. However, this difference is not significant due to the minor impact of VTI anisotropy on very small angles of reflection (less than $2°$ in our case) (Liu and Martinez, 2012).

Regarding lower correlation observed for v_x, it can be attributed to our assumption of a completely horizontal medium, whereas the study area exhibits an approximate dip of $4°$. The obtained results lead us to conclude that for performing a full wave inversion on the land seismic data acquired in the Isleño field, it is advisable to use anisotropic full wave inversion to achieve improved outcomes.

CONCLUSIONS

The results obtained from the numerical modeling demonstrate similarities in the decay of the signal between the real and simulated data for the vertical component (vz). The prediction accuracy for the vertical component (vz) is higher, with correlations in the area of interest for direct waves exceeding 0.75. These correlations indicate a good agreement in both amplitudes and the peaks and valleys. However, for the primary reflected waves, the correlation factor is significantly lower. In the case of the horizontal component (vx), the correlation for direct waves exceeds 0.34, while for the primary reflected waves, the correlation is close to zero (0.10), indicating only a reasonable match in amplitudes but not in the peaks and valleys. Comparing the simulations for an isotropic medium and a VTI anisotropic medium in terms of direct waves, the correlation factor figures suggest that the results for the VTI anisotropic medium are slightly better than those for the isotropic medium. This observation can be attributed to the nearly vertical orientation of the zero-offset VSP, resulting in small incidence angles. While the isotropic full wave inversion performed in this simulation yielded satisfactory results, it is recommended that an anisotropic full wave inversion be employed for the land seismic data of the Isleño field. This is because we anticipate the results to vary significantly due to the inclusion of larger angles present in the land seismic data compared to the angles encountered in this simulation. An anisotropic full wave inversion is better suited for handling these varying angles and is expected to provide more accurate subsurface structural characterization.

ACKNOWLEDGMENTS

The authors would like to thank the authorities of the Petrodelta Joint Company, a subsidiary of Petróleos de Venezuela S.A. (PDVSA) for their collaboration in providing the data for this research.

REFERENCES

Bretaudeau, F., D. Leparoux, O. Durand, and O. Abraham, 2011, Small-scale modeling of onshore seismic experiment: A tool to validate numerical modeling and seismic imaging methods: Geophysics, **76**, T101–T112, doi: 10.1190/geo2010-0339.1.

Burschil, T., T. Beilecke, and C. M. Krawczyk, 2015, Finite-difference modelling to evaluate seismic P-wave and shear-wave field data: Solid Earth, **6**, 33–47, doi: 10.5194/se-6-33-2015.

Caicedo, M. I., and P. Mora, 2004, Temas de propagación de ondas: Universidad Simón Bolívar, Caracas.

Chávez-García, F. J., D. Raptakis, K. Makra, and K. Pitilakis, 2000, Site effects at Euroseistest — ii. results from 2D numerical modeling and comparison with observations: Soil Dynamics and Earthquake Engineering, **19**, 23–39, doi: 10.1016/S0267-7261(99)00026-3.

CVET, 1970, Léxico estratigráfico de venezuela, 2 ed. Boletín de Geología, Publicaciones Especiales.

Etgen, J. T., 1988, Finite-difference elastic anisotropic wave propagation: Technical Report SEP-56, Stanford Exploration Project.

Kelly, K. R., R. W. Ward, S. Treitel, and R. M. Alford, 1976, Synthetic seismograms: A finite-difference approach: Geophysics, **41**, 2–27, doi: 10.1190/1.1440605.

Kormann, J., P. Cobo, B. Biescas, V. Sallarès, C. Papenberg, M. Recuero, and R. Carbonell, 2010, Synthetic modelling of acoustical propagation applied to seismic oceanography experiments: Geophysical Research Letters, **37**, L00D90, doi: 10.1029/2009GL041763.

Li, Y., 2006, An empirical method for estimation of anisotropic parameters in clastic rocks: The Leading Edge, **25**, 706–711, doi: 10.1190/1.2210052.

Liu, E., and A. Martinez, 2012, Fundamentals of seismic anisotropy, *in* Seismic Fracture Characterization: EAGE, 2, 29–57.

Madariaga, R., 1976, Dynamics of an expanding circular fault: Bulletin of the Seismological Society of America, **66**, 639–666, doi: 10.1785/BSSA0660030639.

Pageot, D., D. Leparoux, M. Le Feuvre, O. Durand, P. Cote, and Y. Capdeville, 2017, Improving the seismic small-scale modeling by comparison with numerical methods: Geophysical Journal International, **211**, 637–649, doi: 10.1093/gji/ggx309.

Solymosi, B., N. Favretto-Cristini, V. Monteiller, D. Komatitsch, P. Cristini, B. Arntsen, and B. Ursin, 2018, How to adapt numerical simulation of wave propagation and ultrasonic laboratory experiments to be comparable? a case study for a complex topographic model: Geophysics, **83**, 1–62, doi: 10.1190/geo2017-0536.1.

Tarantola, A., 2005, Inverse problem theory and methods for model parameter estimation: Society for Industrial and Applied Mathematics (SIAM).

Thomsen, L., 1986, Weak elastic anisotropy: Geophysics, **51**, 1954–1966, doi: 10.1190/1.1442051.

Virieux, J., 1986, P-SV wave propagation in heterogeneous media: Velocity-stress finite-difference method: Geophysics, **51**, 889–901, doi: 10.1190/1.1442147.

Yilmaz, O., 2001, Seismic data analysis: Processing, inversion, and interpretation of seismic data, 2 ed. Investigations in Geophysics: Society of Exploration Geophysicists.

Perez-Roa, R.: mathematical development, programming, data preparation and processing, bibliographic review, writing – original draft, writing – review; **Caicedo, M.:** supervision of the research, mathematical development, bibliographic review, result discussion, text revision; **Lagrave, G.:** data preparation, revision, text discussion.

Received on January 9, 2023 / Accepted on November 30, 2023